Journal of
Materials Chemistry A

Accepted Manuscript

This article can be cited before page numbers have been issued, to do this please use: Y. Xu, S. Yin, C. Li, K. Deng, H. Xue, X. Li, H. Wang and L. Wang, *J. Mater. Chem. A*, 2017, DOI: 10.1039/C7TA09939H.

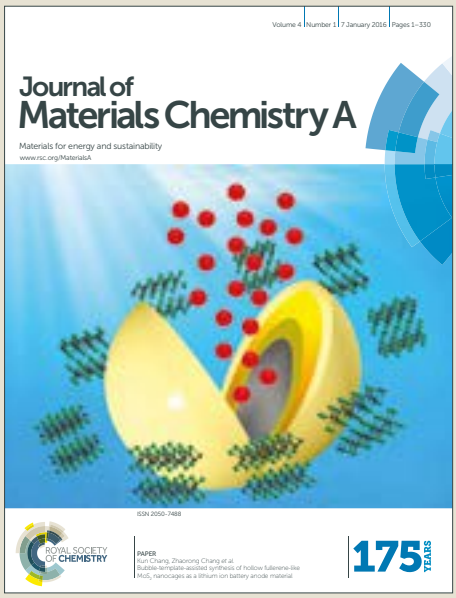

ROYAL SOCIETY OF CHEMISTRY

rsc.li/materials-a

View Article Online
DOI: 10.1039/C7TA09939H

Journal Name

COMMUNICATION

Low-Ruthenium-Content NiRu Nanoalloys Encapsulated in Nitrogen-Doped Carbon as Highly Efficient and pH-Universal Electrocatalysts for Hydrogen Evolution Reaction

Received 00th January 20xx,
Accepted 00th January 20xx

DOI: 10.1039/x0xx00000x

www.rsc.org/

You Xu, Shuli Yin, Chunjie Li, Kai Deng, Hairong Xue, Xiaonian Li, Hongjing Wang,* and Liang Wang*

Rational design and synthesis of low-cost and robust electrocatalysts for hydrogen evolution reaction (HER) is critical for the development of water electrolysis technology. In this work, low-ruthenium-content NiRu alloy nanoparticles encapsulated in nitrogen-doped carbon (NiRu@N-C) have been prepared through doping ruthenium species into nickel-based metal-organic frameworks followed by pyrolysis treatment. Benefiting from the unique structural advantages and synergic effect of the components, the as-obtained NiRu@N-C nanohybrids exhibited excellent electrocatalytic activity and good stability towards HER in acidic, neutral, and alkaline solutions.

Hydrogen is a promising energy carrier towards the sustainable energy economy, and electrocatalytic water-splitting is considered as one of the convenient routs for scale hydrogen generation in high purity.[1-4] One of the key problems for this method is seeking highly active, low-cost, and durable electrocatalysts for the hydrogen evolution reaction (HER).[5-7] So far, platinum (Pt) remains the state-of-the-art H_2-evolving electrocatalyst with nearly zero overpotential and excellent kinetics for actuating the HER. However, multiple fatal disadvantages of the Pt-based catalysts, such as high cost and scare supply, largely limit their practical applications. Therefore, to fulfill the demands in practical use, there is currently a dire need to develop cost-effective alternatives to precious and low abundant Pt material for the HER. In this regard, plenty of non-noble-metal materials, especially transitional metal compounds(e.g., chalcogenides,[8-17] phosphides,[18-27] carbides,[28-31] nitrides[32, 33]), metal-free carbon-based materials,[34-36] and their hybrids[37-44] with various structures and architectures, have been prepared and examined as effective HER catalysts in a series of recent studies. Nevertheless, in most of these cases, their catalytic activity and stability still needs to be improved to compete with Pt-based electrocatalysts.

College of Chemical Engineering, Zhejiang University of Technology, Hangzhou 310014, Zhejiang, P. R. China. E-mail: hjw@zjut.edu.cn, wangliang@zjut.edu.cn
Electronic Supplementary Information (ESI) available: Experimental section and supplementary figures and tables. See DOI: 10.1039/x0xx00000x

Recent advanced studies highlighted that nanocomposites or nanohybrids core-shell structures composed of 3d transitional metals (or their alloys) and N-doped carbon material (M@N-C) hold great promise as substitutes of noble metal electrocatalysts for HER and (or) oxygen evolution reaction (OER) due to the interaction and synergy of the metallic core and carbon shell.[45-51] Such kind of catalysts can have their particular advantages in electrocatalysis applications. Firstly, the carbon shell in such M@N-C core-shell structure could effectively protect the metallic cores from corrosion and aggregation during electrocatalysis processes. Secondly, the doping nitrogen atoms in carbon matrix could modulate the electronic properties of the adjacent carbon atoms by intramolecular charge transfer, which is favourable for improving the electrocatalytic performance. Thirdly, more importantly, the interaction and synergy of metallic core and N-doped carbon shell could create sufficient localized reactive sites by modifying the charge distribution on carbon layer surface via the promoted electron transfer effect, which changes the local work function for related reactive species adsorption and consequently facilitates the HER or OER. It is reported that alloying Co with less noble metal (Ru) could remarkably enhance the catalytic performance of this kind of M@N-C electrocatalysts.[45] This points to the possibility to access new and efficient HER catalysts by combining the Ru-based alloy and carbon materials. Despite these advances, most of the reported M@N-C electrocatalysts could function only in an acidic or basic electrolyte, which limits their applications in different water electrolysis technologies with different demand on the pH value of electrolyte. Therefore, it is highly desirable yet challenging to design and fabricated active H_2-evolving electrocatalysts that exhibit high performance for HER in a wide pH range.

Metal–organic frameworks (MOFs), as a class of porous inorganic-organic hybrid crystals with tunable chemical composition and structure, have been widely used as precursors/sacrificial templates for controllable fabrication of many kinds of carbon-contained composite micro/nano-structures.[52-57] In most early studies, conventional MOF

View Article Online
DOI: 10.1039/C7TA09939H

materials have been commonly used as precursors for being converted into inorganic functional materials via pyrolysis or chemical reaction with desirable reagents. In addition to using simple MOFs as precursors, postsynthetic modification or functionalization of MOFs into novel multicompositional MOF-based analogues could be used to construct complex nanostructured materials with designable structures and compositions via further chemical transformation, which would offer potential possibility to tailor their properties.[45, 58, 59] In the present work, we report the preparation of low-ruthenium-content NiRu alloy nanoparticles encapsulated in N-doped carbon (denote as NiRu@N-C) by coupling with Ru-doping and further pyrolysis treatment under inert atmosphere using a Ni-based MOF as the starting materials (Fig. 1). Benefiting from the structural advantages and component synergy, the as-obtained NiRu@N-C nanohybrids exhibited excellent electrocatalytic activity and good stability towards HER in a wide pH range. Remarkably, the HER activities of optimized NiRu@N-C sample (S-2) in acid and alkaline conditions, featuring with low overpotentials and small Tafel slopes, are comparable with commercially available Pt/C catalyst.

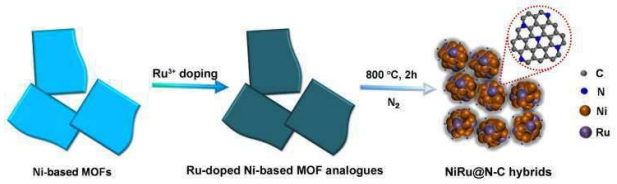

Fig. 1 Schematic of the preparation of NiRu@N-C nanohybrids.

The Ni-based MOF (Ni_2-$(bdc)_2$ted) was first synthesized according to the previous works with some modifications by reacting $Ni(NO_3)_2 \cdot 6H_2O$, bdc(1,4-benzenedicarboxylic acid) and ted(triethylenediamine) in DMF solution under 130 °C for 24 h(see the experimental section for the details, ESI†).[60, 61] Fig. 2a presented the typical scanning electron microscopy (SEM) image of the as-synthesized Ni-based MOF, from which many sheet-like structures with a lateral size of 300~800 nm and a thickness of 20~30 nm can be observed. After further reacting with $RuCl_3$ solution, the sheet-like morphology of the original Ni-based MOF was generally maintained except that the surface become slightly rough, as displayed in Fig. 2b. The as-obtained Ru-doped Ni-based MOF analogues were used as the starting materials for further pyrolysis treatment at 800 °C under a nitrogen flow (see the Experimental Section for the details). A series of NiRu@N-C samples with different Ru contents were obtained by using Ru-doped Ni-based MOF analogues with different doped concentration as the pyrolysis precursors. The as-obtained products are denoted as S-0, S-1, S-2, and S-3, respectively, according to their Ru contents (Table S1, ESI†). Fig. 2c is a representative SEM image of S-2 sample. It was found that numerous irregular particle-like nanostructures with the diameters of 10~20 nm were obtained after annealing treatment. Further transmission electron microscopy (TEM) analysis indicates that these irregular particle-like nanostructures consist of NiRu alloy nanoparticle cores that are coated by ultrathin carbon shells (Fig. 2d and Fig. 2e). The high resolution TEM (HRTEM) image gives clear crystal planes with a d-spacing of 0.21 nm, which can be readily indexed to the (111) crystal plane of the face centred cubic (*fcc*) Ni phase (Fig. 2f). From the HRTEM image, no lattice fringe spaces of metallic Ru were found, implying the formation of NiRu alloy which kept the crystal structure of metallic Ni. Moreover, we can clearly observe that the inner alloy nanoparticles were surrounded by 2~5 layers of graphene shell with an interlayer distance of 0.34 nm (Fig. 2f). The S-0, S-1, and S-3 samples possessed similar morphology and structure to that of S-2 (Fig. S1, ESI†). Energy dispersive X-ray (EDX) spectra show the presence of Ni, Ru, C, and N in these annealed products (Fig. S2, ESI†). The composition of the nanoparticles was further examined by the scanning TEM–energy dispersive X-ray spectroscopy (STEM-EDX), revealing homogeneous distribution of Ni and Ru elements in the inner particles, further confirming the formation of bimetallic NiRu alloy nanoparticles (Fig. 2g-i). The Ru content in S-2 was detected to 1.86 wt% by inductively coupled plasma atomic emission spectrometry (ICP-AES) (Table S2, ESI†).

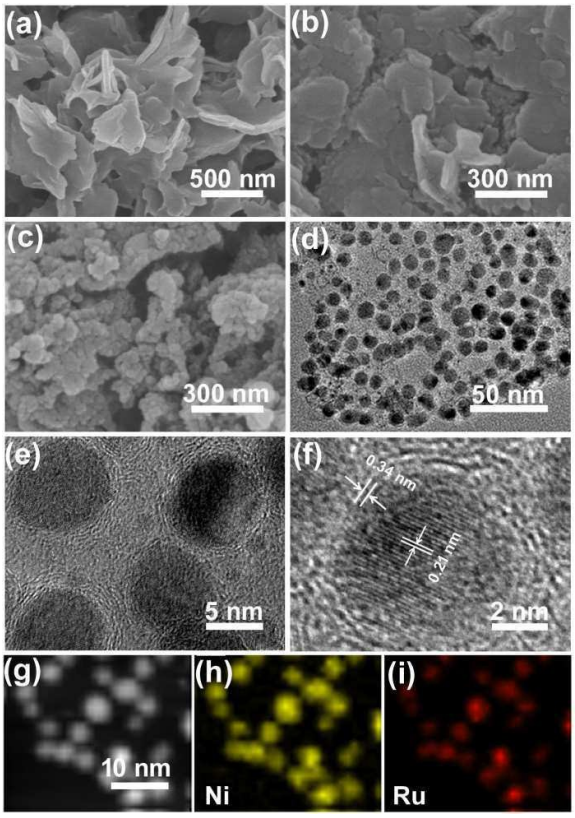

Fig.2 (a) SEM image of Ni-based MOFs. (b) SEM image of Ru-doped Ni-based MOF analogues. (c) SEM image of typical NiRu@N-C (S-2 sample). (d, e) TEM images, (f) HRTEM image and (g-i) HAADF-STEM images and corresponding EDX mappings of Ni (h) and Ru (i) of S-2 sample.

The corresponding X-ray diffraction (XRD) pattern of S-2 sample was shown in Fig. 3a. The very weak and broad C (002)

View Article Online
DOI: 10.1039/C7TA09939H

peak also confirmed that grapheme shells with an ultrathin thickness have been formed, which was in agreement with the result from HRTEM analysis. Besides, the XRD pattern of the S-2 sample showed no additional reflections except a series of Bragg reflections corresponding to the diffractions from NiRu alloy (Fig. 3a). From the Raman spectrum of S-2 sample, two characteristic peaks of graphene with intensity maxima at about 1350 (D band) and 1580 cm^{-1} (G band) were observed, further confirming the presence of graphene shell (see the inset in Fig. 3a). Further information on the composition was obtained by X-ray photoelectron spectroscopy (XPS). The survey XPS spectrum indicated the presence of Ni, Ru, C and N elements (Fig. S3, ESI†). The Ni 2p XPS spectrum reveals that Ni in S-2 sample maintained its metallic state, which was consistent with the XRD and HRTEM results (Fig. 3b). High-resolution XPS spectrum in the C 1s and Ru 3d region are displayed in Fig. 3c. The C 1s peak can be deconvoluted into two peaks centered at 284.7 and 285.9 eV, corresponding to the C-C and C-N bonds, respectively.[62, 63] The Ru 3d peaks at 280.2 and 284.4 eV were assigned to Ru 3d 5/2 and Ru 3d 3/2 for Ru^0.[5, 64] Furthermore, as shown in Fig. 3d, three peaks in the N 1s spectrum of S-2 sample are assigned to pyridinic N (398.7 eV), pyrrolic N (400.5 eV), and graphitic N(402.3 eV), respectively.[62, 63] These results suggested that NiRu@N-C composed of bimetallic NiRu nanoalloy cores and ultrathin N-doped carbon shell have successfully synthesized through doping ruthenium species into Ni-based MOFs followed by pyrolysis treatment.

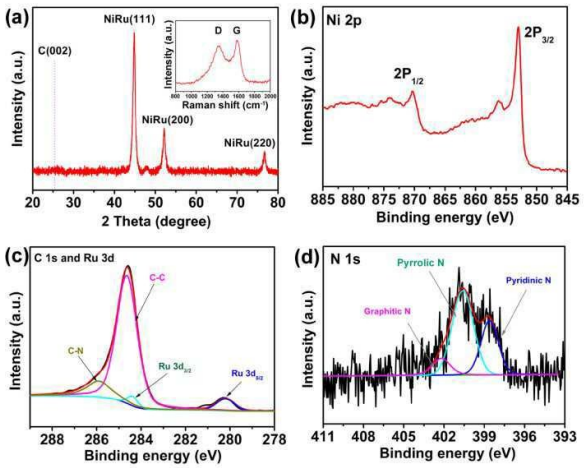

Fig. 3 Structural analysis of typical RuNi@N-C nanohybrid (S-2 sample). (a) XRD. The inset of (a) is Raman spectrum. (b) XPS spectrum of Ni 2p. (c) XPS spectrum of C 1s and Ru 3d. (d) XPS spectrum of N 1s.

During the pyrolysis treatment process under nitrogen atmosphere, Ni^{2+} and Ru^{3+} cations from the Ru-doped Ni-MOF analogues were in situ reduced to form the bimetallic RuNi alloy nanocrystals. Meanwhile, the organic components (*i.e.*, bdc, ted) in the precursor could provide carbon and nitrogen sources for the formation of nitrogen-doped graphene layers surrounding the RuNi alloy nanocrystals, which is able to efficiently avoid the agglomeration of the inside alloy nanoparticles. In such a process, the presence of in-situ formed metal particles could help greatly improve the crystallinity and electrical conductivity of nitrogen-doped graphene layers by catalytic graphitization, which in turn function to efficiently avoid the agglomeration of the inside alloy nanoparticles.

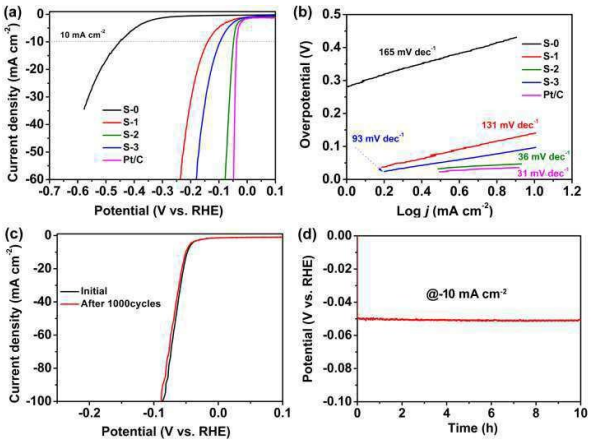

Fig. 4 Electrochemical evaluation of the as-obtained NiRu@N-C series electrocatalysts in 0.5 M H_2SO_4. (a) Polarization curves of various NiRu@N-C and commercial 20 wt% Pt/C catalysts. (b) Tafel plots of various various NiRu@N-C and commercial 20 wt% Pt/C catalysts. (c) Polarization curves of S-2 catalyst decorated GC electrode before and after 1000 CV cycles. (d) Chronopotentiometry test of S-2 catalyst decorated GC electrode held at a constant current density of 10 mA cm^{-2} for 10 h. The polarization curves in (a) and (c) were *iR*-corrected. S-0 represents for Ni@N-C catalysts; S-1, S-2 and S-3 represent for NiRu@N-C catalysts with various Ru contents.

Inspired by the unique alloy-carbon core-shell structure of these as-fabricated NiRu@N-C nanohybids and the attractive electrochemical properties of other reported M@N-C analogues, we studied their electrocatalytic activity towards HER at various pH values by loading them on a polished glassy carbon (GC) electrode and using a three-electrode electrochemical cell system. The HER electrocatalytic activity of NiRu@N-C series electrocatalysts was first investigated in acidic media (0.5 M H_2SO_4, pH=0). The catalytic performance of commercial available Pt/C (20 wt %, Johnson Matthey) was also examined for a comparison. Fig. 4 shows the electrocatalytic activity of various electrocatalysts in 0.5 M H_2SO_4 electrolyte. As expected, Pt/C catalyst-decorated GC electrode exhibited high HER catalytic activity with negligible overpotential and a low Tafel slope of about 31 mV dec^{-1}, which is consistent with the reported values in literatures.[5, 18] It was found that the undoped S-0 sample, that is Ni@N-C obtained by direct pyrolysis of Ni-based MOF, exhibited a poor HER activity with an overpotential of about 450 mV to yield a current density of 10 mA cm^{-2}, which is far inferior to the doped counterparts of NiRu alloy encapsulated in N-doped graphene layers (Fig. 4a). These results suggested the introduction of a suitable amount of Ru into Ni could boost the electrocatalysis activity in such material system, mainly due to higher efficiency of electron transfer from alloy core to graphene shell and enhanced carbon-hydrogen bond in such a alloy-carbon core-shell structure[45]. Among the NiRu@N-C series catlysts, S-2 sample exhibited the best activity among

View Article Online
DOI: 10.1039/C7TA09939H

various NiRu@N-C samples, which is much better than undoped S-0 and other two doped samples (S-1 and S-3). In view of these NiRu@N-C samples vary in Ru content (Table S2, ESI†), the better performance of S-2 catalyst may be contributed to its stronger electronic coupling of Ni and Ru or interatomic charge polarization in it, as explained in the literature[65]. Moreover, the HER activity of S-2 catalyst is also superior to that of NiRu@C counterpart which has similar alloy-carbon core-shell structure but no N-doping atoms in the carbon shell (Fig. S5a-c, ESI†). The required overpotential to achieve a 10 mA cm^{-2} current density was 50 mV with a Tafel slope of 36 mV dec^{-1}(Fig. 4a and b), which is close to commercially available Pt/C catalyst. Notably, these values of the optimized S-2 samples were better than those of many other reported Ni-based HER electrocatalysts in acidic electrolyte, such as $Ni_{0.85}Se$ (~240 mV, 49.3 mV dec^{-1}),[12] Ni_2P (~120 mV, ~46 mV dec^{-1}),[23] CoNi@NC (142 mV, 104 mV dec^{-1}),[48] Mo_xC-Ni@NCV(75 mV, 45 mV dec^{-1}),[42] Fe-Ni_3C (178 mV, 36.5 mV dec^{-1})[31]. Electrochemical impedance spectra (EIS) were employed to study the interfacial electrons transfer dynamics of these NiRu@N-C catalysts. As displayed in Fig. S6a (ESI†), compared to S-0 and other NiRu@N-C catalysts (S-1 and S-3), the S-2 catalyst has the lowest charge-transfer resistance, indicating its superior charge transport kinetics. Moreover, it was found that S-2 catalyst also exhibited high efficient HER activities in acid media when using graphite rod as the counter electrode (Fig. S7, ESI†). These results reveal that the enhanced HER performance is contributed to the intrinsic excellent catalytic activity of the S-2 catalyst.

Durability and stability are another two important criteria to evaluate the performance of an electrocatalyst especially for practical applications. We choose the optimal S-2 sample as the model catalyst to evaluate the durability and stability. Durability of the catalytic response was evaluated by cycling the S-2 decorated GC electrode between +0.1 and -0.09 V (vs. RHE) continuously for 1000 cyclic voltammetry (CV) cycles. After 1000 cycles, the polarization curve of the S-2 sample decorated GC electrode nearly overlaps with the initial one, indicating a superior durability (Fig. 4c). To assess the long-term stability, we carried out chronopotentiometry test at a constant current density of 10 mA cm^{-2} for 10 h. As shown in Fig. 4d, the overpotential of S-2 catalyst decorated GC electrode remained almost constant during the testing, revealing an excellent catalytic stability. It is believed that the superior catalytic stability and durability was ascribed to the structure and morphology stability of these NiRu@N-C catalysts, as analyzed by TEM (Fig. S4, ESI†)

Aiming to make the electrocatalytic H_2 evolution into large scale applications, it is of significance to develop the electrocatalysts with high performance and good stability in the wide pH range of aqueous media. We further evaluated the HER performance of the NiRu@N-C electrocatalysts in alkaline electrolyte(1.0 M KOH, pH=14). As shown in Fig. 5a, S-2 sample exhibited the best electrocatalytic activity among various NiRu@N-C samples. Moreover, the HER activity of S-2 catalyst was also better than that of NiRu@C catalyst in alkaline media (Fig. S5d, ESI†), indicating that the doping N atoms in carbon shell is favourable for improving HER activity. The HER polarization curves of S-2 sample achieved a 10 mA cm^{-2} current density at a low overpotential of 32 mV, which was almost as low as that of Pt/C catalyst. This overpotential was also lower than the values of the currently most promising Ni-based HER electrocatalysts in alkaline medium, such as Ni-$0.2NH_3$(~52 mV),[60] $Ni_{0.95}Co_{0.05}PS_3$(77 mV),[66] NiCu@C (74 mV),[67] Ni_2P (290 mV)[24]. The corresponding Tafel slope of S-2 decorated GC electrode was measured to be 64 mV dec^{-1} (Fig. 5b). Electrochemical impedance characterization revealed a decreased transport resistance of S-2 catalyst compared to S-0, S-1 and S-3 catalysts (Fig. S6b, ESI†). As shown in Fig. 5c, for the durability testing of S-2 electrocatalyst, negligible differences can be observed even after 1000 CV cycles. The excellent long-term catalytic stability was also confirmed by the chronopotentiometry testing at a 10 mA cm^{-2} current density for 10 h (Fig. 5d).

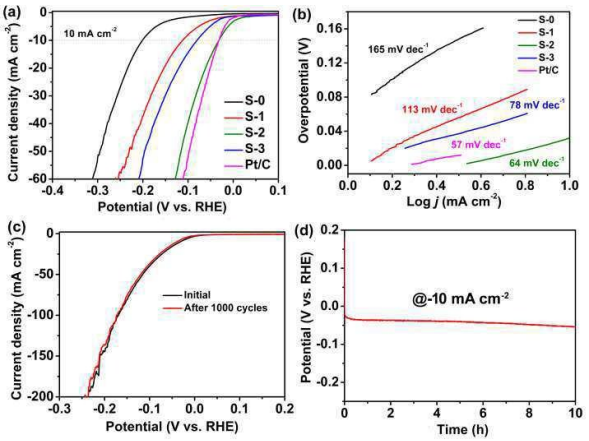

Fig. 5 Electrochemical evaluation of the as-obtained NiRu@N-C series electrocatalysts in 1.0 M KOH. (a) Polarization curves of various NiRu@N-C and commercial 20 wt% Pt/C catalysts. (b) Tafel plots of various various NiRu@N-C and commercial 20 wt% Pt/C catalysts. (c) Polarization curves of S-2 catalyst decorated GC electrode before and after 1000 CV cycles. (d) Chronopotentiometry test of S-2 catalyst decorated GC electrode held at a constant current density of 10 mA cm^{-2} for 10 h. The polarization curves in (a) and (c) were *iR*-corrected. S-0 represents for Ni@N-C catalysts; S-1, S-2 and S-3 represent for NiRu@N-C catalysts with various Ru contents.

Inspired by the high catalytic activity of these NiRu@N-C catalysts in acidic and alkaline conditions, we further studied their electrocatalytic response towards HER in 1.0 M phosphate buffer solution (PBS) (pH=7). As observed from the polarization curves, to drive current densities of 1 and 10 mA cm^{-2}, the best S-2 catalyst decorated GC electrode required overpotentials of 35 and 482 mV, respectively (Fig. S8a, ESI†). HER proceeding in neutral media sustains slower kinetics as compared to that of alkaline and acidic conditions mainly because of larger Ohmic loss, slower ion migration rate and lower proton concentration.[41] Also, the good durability and stability of under neutral condition is confirmed by cycling the S-2 catalyst-decorated GC electrode continuously for 1000 CV cycles and chronoamperometric measurement at 10 mA cm^{-2} for 40 h (Fig. S8b, ESI†). These above results indicated that, by optimizing the structure and composition parameters, these

View Article Online
DOI: 10.1039/C7TA09939H

as-prepared NiRu@N-C series electrocatalysts could exhibit a robust catalytic activity towards HER in aqueous reaction media over a wide pH range.

As for the origin of the markedly enhanced HER activity of the optimized NiRu@N-C electrocatalysts, it is believed that the structural advantages and component synergy should have an important effect for improving the reactivity towards HER. First, the carbon shell in such NiRu@N-C core-shell structure could effectively protect the inner NiRu alloy cores from corrosion and aggregation during long-term electrocatalytic measurement. Secondly, the ultrathin thickness of the carbon shell facilitates the electrons transferring from the inner alloy core to the surface of carbon shell for the catalytic reactions. Thirdly, the interaction and synergy of bimetallic alloy core and N-doped carbon shell could create sufficient localized reactive sites by modifying the charge distribution on carbon layer surface and thus change the local work function for related reactive species adsorption and consequently facilitate HER.

In summary, we have successfully fabricated low-ruthenium-content NiRu@N-C nanohybrids by coupling with Ru-doping treatment and further pyrolysis under inert atmosphere using a Ni-based MOF as the starting materials, and further investigated them as a HER electocatalyst. Benefiting from their structural advantages and component synergy, the NiRu@N-C electrocatalysts show high HER catalytic activity and superior stability in a wide pH range. Remarkably, the HER activities of the optimized S-2 sample in acidic and alkaline conditions are comparable with commercially available Pt/C catalyst. The required overpotentials to drive a current density of 10 mA cm^{-2} over S-2 catalysts were only 50 (in 0.5 M H_2SO_4) and 32 mV (in 1.0 M KOH), corresponding to Tafel slopes of 36 (in 0.5 M H_2SO_4) and 64 mV dec^{-1} (in 1.0 M KOH), respectively. The results here might offer a new avenue for the rational design and synthesis of high-efficient and cost-effective electrocatalysts for water splitting and other electrochemical applications.

Acknowledgements

The work was financially supported by the National Natural Science Foundation of China (No. 21601154, 21776255, 21701141), and Natural Science Foundation of Zhejiang Province (No. LQ18B010005).

Notes and references

1 A. Züttel, A. Remhof, A. Borgschulte and O. Friedrichs, *Phil. Trans. R. Soc. A*, 2010, **368**, 3329-3342.
2 X. Zou and Y. Zhang, *Chem. Soc. Rev.*, 2015, **44**, 5148-5180.
3 Y. Xu, M. Kraft and R. Xu, *Chem. Soc. Rev.*, 2016, **45**, 3039-3052.
4 K.-Y. Niu, F. Lin, S. Jung, L. Fang, D. Nordlund, C. C. L. McCrory, T.-C. Weng, P. Ercius, M. M. Doeff and H. Zheng, *Nano Lett.*, 2015, **15**, 2498-2503.
5 J. Mahmood, F. Li, S.-M. Jung, M. S. Okyay, I. Ahmad, S.-J. Kim, N. Park, H. Y. Jeong and J.-B. Baek, *Nat. Nanotechnol.*, 2017, **12**, 441-446.
6 Y. Jiao, Y. Zheng, K. Davey and S.-Z. Qiao, *Nat. Energy*, 2016, **1**, 16130.
7 Z. Xia, *Nat. Energy*, 2016, **1**, 16155.
8 D. Damien, A. Anil, D. Chatterjee and M. M. Shaijumon, *J. Mater. Chem. A*, 2017, **5**, 13364-13372.
9 J. Guo, X. Zhang, Y. Sun, L. Tang and X. Zhang, *J. Mater. Chem. A*, 2017, **5**, 11309-11315.
10 W. Wang, L. Yang, F. Qu, Z. Liu, G. Du, A. M. Asiri, Y. Yao, L. Chen and X. Sun, *J. Mater. Chem. A*, 2017, **5**, 16585-16589.
11 X. Ren, W. Wang, R. Ge, S. Hao, F. Qu, G. Du, A. M. Asiri, Q. Wei, L. Chen and X. Sun, *Chem. Commun.*, 2017, **53**, 9000-9003.
12 B. Yu, Y. Hu, F. Qi, X. Wang, B. Zheng, K. Liu, W. Zhang, Y. Li and Y. Chen, *Electrochim. Acta*, 2017, **242**, 25-30.
13 R. Miao, B. Dutta, S. Sahoo, J. He, W. Zhong, S. A. Cetegen, T. Jiang, S. P. Alpay and S. L. Suib, *J. Am. Chem. Soc.*, 2017, **139**, 13604-13607.
14 S. Dutta, A. Indra, Y. Feng, T. Song and U. Paik, *ACS Appl. Mater. Interfaces*, 2017, **9**, 33766-33774.
15 Z. Pu, Y. Luo, A. M. Asiri and X. Sun, *ACS Appl. Mater. Interfaces*, 2016, **8**, 4718-4723.
16 Y. Guo, J. Tang, H. Qian, Z. Wang and Y. Yamauchi, *Chem. Mater.*, 2017, **29**, 5566-5573.
17 J. Ding, Y. Zhou, Y. Li, S. Guo and X. Huang, *Chem. Mater.*, 2016, **28**, 2074-2080.
18 C. Zhang, Y. Huang, Y. Yu, J. Zhang, S. Zhuo and B. Zhang, *Chem. Sci.*, 2017, **8**, 2769-2775.
19 Y. Xu, R. Wu, J. Zhang, Y. Shi and B. Zhang, *Chem. Commun.*, 2013, **49**, 6656-6658.
20 R. Zhang, X. Wang, S. Yu, T. Wen, X. Zhu, F. Yang, X. Sun, X. Wang and W. Hu, *Adv. Mater.*, 2017, **29**, 1605502.
21 Z.-H. Xue, H. Su, Q.-Y. Yu, B. Zhang, H.-H. Wang, X.-H. Li and J.-S. Chen, *Adv. Energy Mater.*, 2017, **7**, 1602355.
22 J. Li, G. Wei, Y. Zhu, Y. Xi, X. Pan, Y. Ji, I. V. Zatovsky and W. Han, *J. Mater. Chem. A*, 2017, **5**, 14828-14837.
23 E. J. Popczun, J. R. McKone, C. G. Read, A. J. Biacchi, A. M. Wiltrout, N. S. Lewis and R. E. Schaak, *J. Am. Chem. Soc.*, 2013, **135**, 9267-9270.
24 L.-A. Stern, L. Feng, F. Song and X. Hu, *Energy Environ. Sci.*, 2015, **8**, 2347-2351.
25 F. H. Saadi, A. I. Carim, W. S. Drisdell, S. Gul, J. H. Baricuatro, J. Yano, M. P. Soriaga and N. S. Lewis, *J. Am. Chem. Soc.*, 2017, **139**, 12927-12930.
26 X. D. Wang, Y. Cao, Y. Teng, H. Y. Chen, Y. F. Xu and D. B. Kuang, *ACS Appl. Mater. Interfaces*, 2017, **9**, 32812-32819.
27 T. Liu, X. Ma, D. Liu, S. Hao, G. Du, Y. Ma, A. M. Asiri, X. Sun and L. Chen, *ACS Catal.*, 2016, **7**, 98-102.
28 F. Li, X. Zhao, J. Mahmood, M. S. Okyay, S. M. Jung, I. Ahmad, S. J. Kim, G. F. Han, N. Park and J. B. Baek, *ACS nano*, 2017, **11**, 7527-7533.
29 C. Wan, Y. N. Regmi and B. M. Leonard, *Angew. Chem. Int. Ed.*, 2014, **53**, 6407-6410.

View Article Online
DOI: 10.1039/C7TA09939H

30 L. Liao, S. Wang, J. Xiao, X. Bian, Y. Zhang, M. D. Scanlon, X. Hu, Y. Tang, B. Liu and H. H. Girault, *Energy Environ. Sci.*, 2014, **7**, 387-392.
31 H. Fan, H. Yu, Y. Zhang, Y. Zheng, Y. Luo, Z. Dai, B. Li, Y. Zong and Q. Yan, *Angew. Chem. Int. Ed.*, 2017, **56**, 12566-12570.
32 B. Cao, G. M. Veith, J. C. Neuefeind, R. R. Adzic and P. G. Khalifah, *J. Am. Chem. Soc.*, 2013, **135**, 19186-19192.
33 W.-F. Chen, K. Sasaki, C. Ma, A. I. Frenkel, N. Marinkovic, J. T. Muckerman, Y. Zhu and R. R. Adzic, *Angew. Chem. Int. Ed.*, 2012, **51**, 6131-6135.
34 Y. Zheng, Y. Jiao, Y. Zhu, L. H. Li, Y. Han, Y. Chen, A. Du, M. Jaroniec and S. Z. Qiao, *Nat. Commun.*, 2014, **5**, 3783.
35 M. Chhetri, S. Maitra, H. Chakraborty, U. V. Waghmare and C. N. R. Rao, *Energy Environ. Sci.*, 2016, **9**, 95-101.
36 J. Zhang, L. Qu, G. Shi, J. Liu, J. Chen and L. Dai, *Angew. Chem. Int. Ed.*, 2016, **55**, 2230-2234.
37 L. Chen, H. Jiang, H. Jiang, H. Zhang, S. Guo, Y. Hu and C. Li, *Adv. Energy Mater.*, 2017, **7**, 1602782.
38 J. Jiang, Q. Liu, C. Zeng and L. Ai, *J. Mater. Chem. A*, 2017, **5**, 16929-16935.
39 X.-Y. Yu, Y. Feng, B. Guan, X. W. Lou and U. Paik, *Energy Environ. Sci.*, 2016, **9**, 1246-1250.
40 J. Deng, P. Ren, D. Deng, L. Yu, F. Yang and X. Bao, *Energy Environ. Sci.*, 2014, **7**, 1919-1923.
41 J. Wang, F. Xu, H. Jin, Y. Chen and Y. Wang, *Adv. Mater.*, 2017, **29**, 1605838.
42 S. Wang, J. Wang, M. Zhu, X. Bao, B. Xiao, D. Su, H. Li and Y. Wang, *J. Am. Chem. Soc.*, 2015, **137**, 15753-15759.
43 T. Q. Zhang, J. Liu, L. B. Huang, X. D. Zhang, Y. G. Sun, X. C. Liu, D. S. Bin, X. Chen, A. M. Cao, J. S. Hu and L. J. Wan, *J. Am. Chem. Soc.*, 2017, **139**, 11248-11253.
44 D. Y. Chung, S. W. Jun, G. Yoon, H. Kim, J. M. Yoo, K. S. Lee, T. Kim, H. Shin, A. K. Sinha, S. G. Kwon, K. Kang, T. Hyeon and Y. E. Sung, *J. Am. Chem. Soc.*, 2017, **139**, 6669-6674.
45 J. Su, Y. Yang, G. Xia, J. Chen, P. Jiang and Q. Chen, *Nat. Commun.*, 2017, **8**, 14969.
46 Y. Yang, Z. Lin, S. Gao, J. Su, Z. Lun, G. Xia, J. Chen, R. Zhang and Q. Chen, *ACS Catal.*, 2017, **7**, 469-479.
47 Y. Xu, W. Tu, B. Zhang, S. Yin, Y. Huang, M. Kraft and R. Xu, *Adv. Mater.*, 2017, **29**, 1605957.
48 J. Deng, P. Ren, D. Deng and X. Bao, *Angew. Chem. Int. Ed.*, 2015, **54**, 2100-2104.
49 L. Du, L. Luo, Z. Feng, M. Engelhard, X. Xie, B. Han, J. Sun, J. Zhang, G. Yin, C. Wang, Y. Wang and Y. Shao, *Nano Energy*, 2017, **39**, 245-252.
50 Y.-Y. Ma, C.-X. Wu, X.-J. Feng, H.-Q. Tan, L.-K. Yan, Y. Liu, Z.-H. Kang, E.-B. Wang and Y.-G. Li, *Energy Environ. Sci.*, 2017, **10**, 788-798.
51 Y. Yang, Z. Lun, G. Xia, F. Zheng, M. He and Q. Chen, *Energy Environ. Sci.*, 2015, **8**, 3563-3571.
52 X. Cao, C. Tan, M. Sindoro and H. Zhang, *Chem. Soc. Rev.*, 2017, **46**, 2660-2677.
53 K. Shen, X. Chen, J. Chen and Y. Li, *ACS Catal.*, 2016, **6**, 5887-5903.
54 J. Liu, D. Zhu, C. Guo, A. Vasileff and S.-Z. Qiao, *Adv. Energy Mater.*, 2017, DOI: 10.1002/aenm.201700518, 1700518.
55 Y. V. Kaneti, S. Dutta, M. S. A. Hossain, M. J. A. Shiddiky, K. L. Tung, F. K. Shieh, C. K. Tsung, K. C. Wu and Y. Yamauchi, *Adv. Mater.*, 2017, **29**, 1700213.
56 S. Fu, C. Zhu, J. Song, D. Du and Y. Lin, *Adv. Energy Mater.*, 2017, **7**, 1700363.
57 K. Niu, Y. Xu, H. Wang, R. Ye, H. L. Xin, F. Lin, C. Tian, Y. Lum, K. C. Bustillo, M. M. Doeff, M. T. M. Koper, J. Ager, R. Xu and H. Zheng, *Sci. Adv.*, 2017, **3**, e1700921.
58 C. Zhao, X. Dai, T. Yao, W. Chen, X. Wang, J. Wang, J. Yang, S. Wei, Y. Wu and Y. Li, *J. Am. Chem. Soc.*, 2017, **139**, 8078-8081.
59 B. Y. Guan, X. Y. Yu, H. B. Wu and X. W. D. Lou, *Adv. Mater.*, 2017, DOI: 10.1002/adma.201703614, 1703614.
60 T. Wang, Q. Zhou, X. Wang, J. Zheng and X. Li, *J. Mater. Chem. A*, 2015, **3**, 16435-16439.
61 P. Song, Y. Li, B. He, J. Yang, J. Zheng and X. Li, *Microporous Mesoporous Mater.*, 2011, **142**, 208-213.
62 F. Cao, M. Zhao, Y. Yu, B. Chen, Y. Huang, J. Yang, X. Cao, Q. Lu, X. Zhang, Z. Zhang, C. Tan and H. Zhang, *J. Am. Chem. Soc.*, 2016, **138**, 6924-6927.
63 S. Yang, L. Zhi, K. Tang, X. Feng, J. Maier and K. Müllen, *Adv. Funct. Mater.*, 2012, **22**, 3634-3640.
64 W. Cao, W. Luo, H. Ge, Y. Su, A. Wang and T. Zhang, *Green Chem.*, 2017, **19**, 2201-2211.
65 C. Zhang, Y. Liu, Y. Chang, Y. Lu, S. Zhao, D. Xu, Z. Dai, M. Han and J. Bao, *ACS Applied Materials & Interfaces*, 2017, **9**, 17326-17336.
66 K. Li, D. Rakov, W. Zhang and P. Xu, *Chem. Commun.*, 2017, **53**, 8199-8202.
67 Y. Shen, Y. Zhou, D. Wang, X. Wu, J. Li and J. Xi, *Adv. Energy Mater.*, 2017, DOI: 10.1002/aenm.201701759, 1701759.

View Article Online
DOI: 10.1039/C7TA09939H

Graphical Abstract

NiRu@N-C hybrid is fabricated and tested as an efficient catalyst for hydrogen evolution reaction in a wide pH rang.